PHYSICAL REVIEW LETTERS **127,** 204501 (2021)

Editors' Suggestion Featured in Physics

Triple Leidenfrost Effect: Preventing Coalescence of Drops on a Hot Plate

F. Pacheco-Vázquez,[1,*] R. Ledesma-Alonso,[2,†] J. L. Palacio-Rangel,[1] and F. Moreau[3]
[1]*Instituto de Física, Benemérita Universidad Autónoma de Puebla, A. P. J-48, Puebla 72570, Mexico*
[2]*Universidad de las Américas Puebla, San Andrés Cholula, C.P. 72810, Puebla, Mexico*
[3]*Institut Pprime, UPR 3346 CNRS, ENSMA, Université de Poitiers, BP 40109, F-86961 Futuroscope Cedex, France*

(Received 19 February 2021; revised 9 August 2021; accepted 6 October 2021; published 12 November 2021)

We report on the collision-coalescence dynamics of drops in Leidenfrost state using liquids with different physicochemical properties. Drops of the same liquid deposited on a hot concave surface coalesce practically at contact, but when drops of different liquids collide, they can bounce several times before finally coalescing when the one that evaporates faster reaches a size similar to its capillary length. The bouncing dynamics is produced because the drops are not only in Leidenfrost state with the substrate, they also experience Leidenfrost effect between them at the moment of collision. This happens due to their different boiling temperatures, and therefore, the hotter drop works as a hot surface for the drop with lower boiling point, producing three contact zones of Leidenfrost state simultaneously. We called this scenario the *triple* Leidenfrost effect.

DOI: 10.1103/PhysRevLett.127.204501

A liquid droplet in Leidenfrost state levitates on its own vapor over a hot surface, reducing its evaporation rate and sliding friction [1,2]. The minimum temperature T_L required to observe such a scenario depends mainly on the liquid and surface properties [3–6]. For instance, a water drop enters in Leidenfrost state on a polished aluminum plate at $T_L \approx 160$–$200\,^{\circ}\mathrm{C}$ [6,7]. In contrast, a slight superheating can be enough to observe levitation of an ethanol droplet on a liquid oil pool [8]. Recently, different Leidenfrost dynamics were explored: self-propulsion [9–12], sustained rotation [13,14], oscillations [7,15,16], inverted Leidenfrost [17], exploding droplets [18], etc. These studies suggest manipulating Leidenfrost droplets for applications in engineering and microfluidics. However, we need to understand first how Leidenfrost drops of different liquids interact [19–22].

When two droplets of the same liquid collide, they coalesce if the gas film between them is drained during the collision time. At room temperature, different regimes of bouncing, coalescence, and separation in two-droplet collisions are well known depending on the Weber number (the ratio of collision energy to surface energy), impact parameter (the deviation of the droplets trajectories from that of head-on impact), and droplets size ratio [23–27]. The dynamics also depends on liquids miscibility [28–30]: a water droplet coalesces with an ethanol droplet [29] but it can bounce against an oil droplet [30]. On nonwetting surfaces, two micrometric droplets may coalesce, bounce, or propel, due to the transfer of surface energy to mechanical energy [31,32]. The temperature effect was recently considered only for water droplets collisions [33–35]: an increase in temperature for both or one of the droplets increases the possibility of coalescence [33], and self-propelled jumping upon coalescence occurs for water droplets in Leidenfrost state [31,34], as in the case of drops on superhydrophobic surfaces [31].

In this Letter, we study for the first time the collision outcome of two Leidenfrost drops of different miscible and immiscible liquids. First, we determine the Leidenfrost temperature T_L for each liquid. Then, we focus on two large drops colliding on a hot concave plate at temperature $T_p > T_L$: the drops coalesce directly or bounce repeatedly depending on the difference of the liquids boiling temperatures ΔT_B, see movie in Supplemental Material [36]. The bouncing dynamics can be explained assuming that the Leidenfrost effect is also established between droplets with large ΔT_B, generating a vapor layer that prevents coalescence. After one droplet evaporates reaching a size similar to its capillary length, the drops finally coalesce regardless of the initial volume, impact velocity, and plate temperature, in the studied ranges. Three scenarios follow the coalescence: miscible droplets quickly mix, immiscible droplets form a multiphasic Leidenfrost drop, and a volatile droplet explodes violently inside a hotter drop.

Experimental setup.—We placed on a hotplate a polished cylindrical aluminum substrate (15 cm diameter, 4 cm thickness, roughness $< 0.5\ \mu$m) machined radially with a small angle ($\phi = 2°$) to keep the droplets on the center of its surface. The plate temperature was controlled with a solid state relay (SSR) and monitored with a K-type ATT29 thermocouple (TC). One or two drops of initial volume $V_0 \in [5, 1000]\ \mu$l of eleven low viscosity liquids with different physicochemical properties (see data in [36]) were deposited on the plate, and the bouncing or coalescence dynamics was filmed from the top with a high speed camera Photron SA3, see Fig. 1.

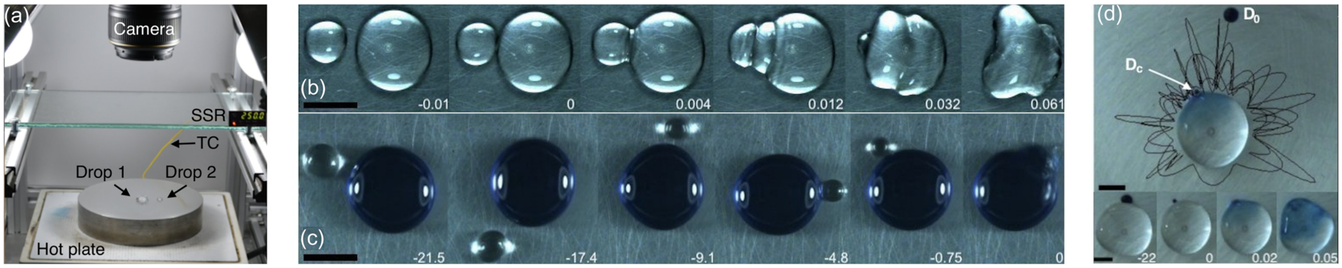

FIG. 1. (a) Experimental setup. (b) Direct coalescence of two water drops in Leidenfrost state. (c) Consecutive bouncing of an ethanol droplet (transparent one) against a water droplet (tinted with methylene blue) during several seconds before coalescing. (d) Path of an acetonitrile droplet (tinted in blue) bouncing several times against a water drop. The snapshots show that the water droplet, initially transparent, turns bluish suddenly when the droplets coalesce. In (b)–(d), the elapsed time is indicated in seconds in each snapshot, with $t = 0$ s corresponding to the moment of coalescence [scale bars: (b) and (c) 10 mm, (d) 5 mm].

One droplet evaporation.—To determine T_L for each liquid, we measured the evaporation time τ of 500 μl droplets at different plate temperatures T_p. An abrupt increase of $\tau(T_p)$ occurs at $T_p \approx T_L$ [2]. In Fig. 2(a), τ vs T_p is reported for water (red squares), in which case $T_L \approx 210\,°\mathrm{C}$. Similar plots were obtained for all liquids but only the values of $\tau(T_L)$ are shown (blue points). In most cases $\tau(T_L) \sim 100$–200 s, but for water $\tau(T_L) \sim 450$ s due to its more than twice larger latent heat L, see Table I. Figure 2(b), shows T_L vs T_B for each liquid. The data can be linearly scaled [see Fig. 2(c)] using the dimensionless temperatures proposed very recently in Ref. [43], given by $\Theta_L = T_L C_p / L$ and $\Theta_B = T_B C_p / L$, where C_p is the gas specific heat. The linear fit (blue line) may provide a good estimate of T_L for an additional liquid deposited on the aluminum plate, if L, C_p, and T_B are known.

Collision of two drops.—Once known T_L for each liquid, two drops of different liquids [labeled Drop 1 and Drop 2 in Fig. 1(a)] with boiling temperatures T_{B1} and T_{B2} were deposited on the aluminum plate at $T_p = 250\,°\mathrm{C}$ ($T_p > T_L$ for both drops [45]). First, we placed Drop 1 of volume $V_0 = 1000\ \mu$l at the center of the plate. Then, Drop 2 of $V_0 \in [100, 700]\ \mu$l was released close to the edge of the plate at $d \sim 7$ cm from Drop 1. Drop 2 slides under the action of gravity g until colliding with Drop 1 with impact velocity $v \sim \sqrt{2gd \sin\phi} \approx 22$ cm/s. The collision is followed by two dynamics depending on the liquids pairs: (i) direct coalescence or (ii) consecutive rebounds before coalescence. The direct coalescence lasts some milliseconds [Fig. 1(b)], and it was observed mainly with drops of the same liquid (e.g., water-water) or liquids with similar properties (e.g., ethanol-isopropanol). In contrast, drops with large differences in properties (e.g., water-ethanol or water-acetonitrile) remain bouncing during several seconds, or even minutes, while they evaporate until reaching a critical size to finally coalesce [Figs. 1(c) and 1(d)]. Table I summarizes our findings based on the dominant dynamics observed in at least five repetitions for each liquid pair.

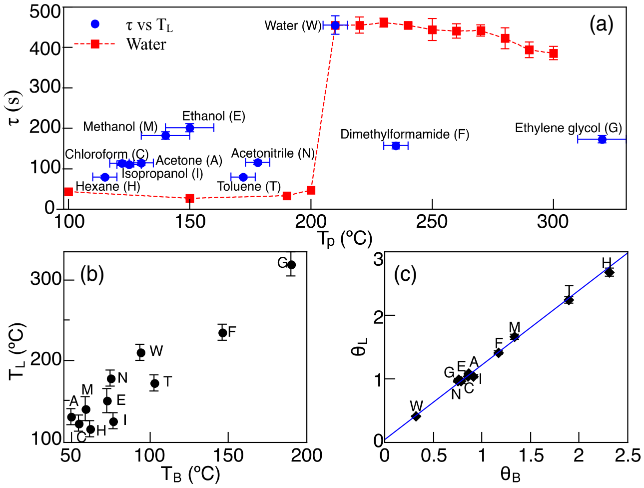

FIG. 2. (a) Evaporation time τ vs plate temperature T_p (red squares) and $\tau(T_L)$ (blue dots), for 0.5 ml drops of different liquids. (b) T_L vs T_B and (c) Θ_L vs Θ_B, for the liquids in (a), with the best linear fit: $\Theta_L = 1.17\Theta_B + 0.05$ (see text).

TABLE I. Outcome of the collision of two Leidenfrost drops for different liquids pairs [44]: direct coalescence (c), consecutive rebound (r), or both scenarios (c/r). A subindex (i) indicates immiscible liquids [37]. The latent heat L, surface tension σ, and capillary length λ_c of each liquid at the boiling temperature T_B are reported (values in Puebla, Mexico, at ~2200 m above the sea level). Data based on Refs. [37–40].

Liquid	T_B °C	L kJ/kg	σ mN/m	λ_c mm	Drop 1	Drop 2									
						W	E	M	I	A	H	C	N	T	F
Water	93	2256	59	2.5	W	c	r	r	r	r	$r_{(i)}$	$r_{(i)}$	r	$c_{(i)}$	c
Ethanol	72	846	17	1.5	E	r	c	c	c	c	r	c	c	r	r
Methanol	59	1100	19	1.6	M	r	c	c	c	c	$r_{(i)}$	r	c	r	r
Isopropanol	76	779	16	1.5	I	r	c	c	c	c	r	c	c	c/r	r
Acetone	50	518	19	1.7	A	r	c	c	c	c	r	c	c/r	r	r
Hexane	61	338	13	1.5	H	$r_{(i)}$	r	$r_{(i)}$	r	r	c	c	$r_{(i)}$	r	$r_{(i)}$
Chloroform	54	247	22	1.3	C	$r_{(i)}$	c	r	c	c	c	c	c	c	r
Acetonitrile	74	729	22	1.8	N	r	c	c	c	c/r	$r_{(i)}$	c	c	c/r	r
Toluene	103	365	18	1.5	T	$c_{(i)}$	r	r	c/r	r	r	c	c/r	c	r
DFormamide	146	546	22	1.6	F	c	r	r	r	r	$r_{(i)}$	r	r	r	c

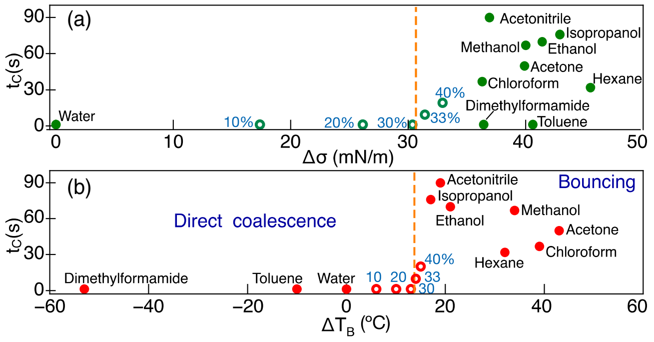

FIG. 3. Coalescence time t_c for a 250 μl Drop 2 of the indicated liquids with a 1 ml Drop 1 of water as a function of (a) $\Delta\sigma$ and (b) ΔT. Blue numbers denote the ethanol concentration (percent) in Drop 2 composed of water-ethanol mixtures.

Note that drops of the same liquid always coalesce directly (main diagonal), almost all liquids bounce against water or dimethylformamide, alcohols coalesce between them, and three pairs can either coalesce or bounce. For immiscible liquids, the drops can bounce (e.g., hexane with water) or merge directly (toluene with water), but at the end the liquids remain unmixed forming a multiphasic Leidenfrost drop.

Let us focus on the experiments with a 1 ml Drop 1 of water interacting with a 250 μl Drop 2 of another liquid (their properties are labeled with a subindices $_1$ and $_2$, respectively). For these combinations, we measured the time t_c from Drop 2 deposition until its coalescence with Drop 1. Then, we realized that two parameters could determine the conditions for direct coalescence ($t_c \sim 0$) or bouncing ($t_c \gg 0$): the difference of surface tensions $\Delta\sigma = \sigma_1 - \sigma_2$, see Fig. 3(a), or the difference in boiling temperatures $\Delta T_B = T_{B1} - T_{B2}$, see Fig. 3(b). Note in these plots the transition from direct coalescence to bouncing at $\Delta\sigma \approx 31$ mN/m, and at $\Delta T_B \approx 15\,^{\circ}$C, respectively (dashed lines). We also performed experiments using mixtures of water and ethanol for Drop 2 (open symbols), reducing progressively $\sigma_2 \approx 59$ mN/m and $T_{B2} \approx 93\,^{\circ}$C for pure water, in which case Drop 2 coalesces directly with Drop 1 (same liquid), until attaining an ethanol concentration of 33%, at which Drop 2 exhibits bouncing before coalescence. For this concentration, $\sigma_2 \approx 28$ mN/m and $T_{B2} \approx 78\,^{\circ}$C [38], which corresponds to $\Delta\sigma \approx 31$ mN/m and $\Delta T_B \approx 15\,^{\circ}$C. These transition values are in agreement with those found using different liquids. One can notice in Fig. 3 that toluene and dimethylformamide (with $t_c \approx 0$ s) are beyond the transition for $\Delta\sigma$ but appear in the right side considering ΔT_B. This suggests that ΔT_B determines if two droplets bounce or coalesce.

Bouncing dynamics and coalescence size.—We performed particle tracking from videos taken at 60 fps focused on Drop 2 bouncing against Drop 1. An example of this dynamics is shown in Fig. 1(d) for acetonitrile bouncing during the last 22 s before coalescing with water. Figure 4(a) shows the radial position of Drop 2, r_b, measured from the surface of Drop 1 for different liquids: isopropanol performs the largest rebounds and chloroform the smallest ones. The erratic bouncing lengths indicate that the moment of coalescence is independent of the impact velocity in the studied range. This also indicates that the rebound velocity can be higher than the impacting velocity, which is possible if the vapor layer is replenished by the evaporation of the Leidenfrost droplets during the collision time [34]. Note the remarkable difference between our results and those found for drops at ambient temperature [29]. If one takes for example the Drop 2 of ethanol (density $\rho = 0.748$ g/cm^3, initial diameter $D_2 \sim 1.5$ cm) that bounces different radial distances with $v \approx 0$–22 cm/s and impact parameter $X \sim 0$, the Weber number, $\mathrm{We} = \rho v^2 D_2/\sigma$, is in the range $0 < \mathrm{We} < 46$. At room temperature and similar Weber numbers, a water drop always coalesces with an ethanol drop [29], whereas in Leidenfrost state, we observed repeated bouncing.

Figure 4(b) shows that, for all liquids, the diameter D_2 of Drop 2 decreases linearly with time due to evaporation until

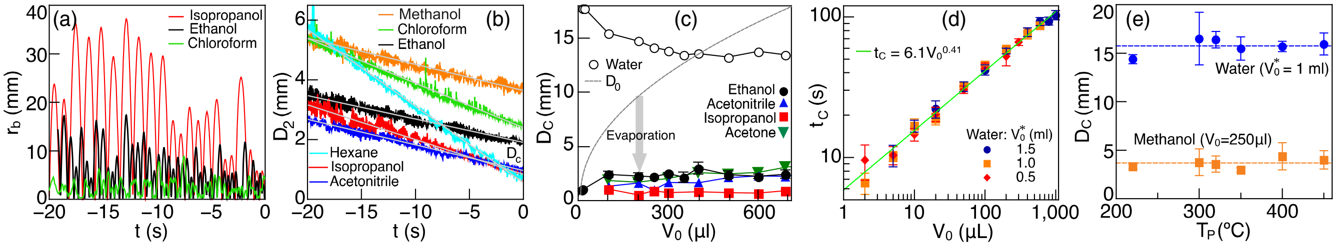

FIG. 4. (a) Radial bouncing distance r_b and (b) diameter D_2 of Drop 2 as a function of time t, for drops of different liquids of initial volume $V_0 = 250$ μl before coalescing with water. For clarity, only the last 20 s of bouncing are shown (coalescence occurs at $t = 0$ s). A complete evolution of $D_2(t)$ can be found in Supplemental Material [36]. In (b), gray lines exhibit the linear decrease of D_2 vs t. (c) Coalescence size D_c of Drop 2 as a function of V_0 for different liquids. For reference, we show D_c for the water Drop 1 (open circles) coalescing with the Drop 2 of ethanol, and the initial diameter D_0 of the latter considering a pancakelike shape (dashed line). (d) Log-log plot of t_c vs V_0 of a Drop 2 of methanol with a water Drop 1 of three different initial volumes V_0^*. The green line highlights a power-law behavior of the form $t_c = aV_0^n$. In (a)–(d), the experiments were performed at $T_p = 250\,^{\circ}$C. (e) D_c for methanol and water drops when they coalesce, as a function of T_p (their respective initial volumes V_0 and V_0^* are indicated).

coalescing at $t = 0$ s, with coalescence size $D_c \sim 1$–3 mm. This linear dependence, with slope $k = -dD_2(t)/dt$ given by the liquid evaporation rate (gray lines), is in agreement with Ref. [8] for the evaporation of a single Leidenfrost drop on a heated liquid pool, and it contrasts with the power-law model derived in Ref. [2] for individual water drops. Furthermore, D_c is largely independent of the initial volume of Drop 2 in the range $V_0 \in [100, 700]$ μl, as shown in Fig. 4(c) (solid symbols). The dashed line indicates the diameter D_0 (viewed from above) of a drop with pancakelike shape and initial volume V_0; the drops evaporate and decrease linearly in size from D_0 until reaching a size D_c, of the order of the liquids capillary lengths, $\lambda_c = (\sigma/\rho g)^{1/2}$ (see values in Table I). Figure 4(d) shows the case of methanol droplets of different initial volumes coalescing with water drops of $V_0^* = 0.5$, 1.0, 1.5 ml. The coalescence time for a given V_0 is the same in the three cases, indicating that t_c only depends on the volume of Drop 2, i.e., when it reaches a given diameter $D_2 = D_c$, regardless of the diameter of the central drop D_1 [the equivalent coalescence diameter is $D_{\mathrm{eq}} = D_1 D_2/(D_1 + D_2)$, since $D_2 \ll D_1$, then $D_{\mathrm{eq}} \sim D_2$, i.e., the smaller drop essentially interacts with a flat surface]. As shown in Fig. 4(d), t_c follows a power-law dependence on V_0 similar to the one described previously for the lifetime of a single Leidenfrost drop [41]. Remarkably, D_c is also independent of T_p (for $T_p > T_L$), as it is shown in Fig. 4(e) for experiments performed in the range of $220\,^{\circ}\mathrm{C} < T_p < 450\,^{\circ}\mathrm{C}$. Although only the case of methanol-water pair is shown in Figs. 4(d) and 4(e), similar results were obtained using other liquids.

The triple Leidenfrost effect.—Based on the above observations, we propose a simple mechanism illustrated in Fig. 5(a) to explain the different collision outcomes for Leidenfrost droplets: when two droplets are deposited on a very hot plate at temperature T_p, both droplets levitate on their own vapor, experiencing independently the well known Leidenfrost effect. The temperature of each droplet is practically its boiling temperature [2]; in the sketch, Drop 1 is at temperature T_{B1}, and Drop 2 at temperature T_{B2}. For two drops of distinct liquids, one drop has a higher boiling point than the other one. Let us say $T_{B1} \gg T_{B2}$. As in the case of droplet levitation on a liquid pool [8], Drop 1 acts as a superheated surface for Drop 2, and consequently, the Leidenfrost state is also established between the droplets, preventing coalescence. Therefore, there are three simultaneous zones of vapor-mediated levitation, indicated by $L1$, $L2$, and $L3$ in Fig. 5(a). This also explains why two droplets of the same liquid coalesce directly, because in such a case $T_{B1} = T_{B2}$ and the Leidenfrost effect between the droplets is not established. Moreover, if ΔT_B is very small, the amount of vapor produced during the collision is not enough to avoid contact [46]. The vapor expelled from the bottom of the droplets cannot be the responsible of the frustrated coalescence for two reasons: (1) if that were the case, two droplets of the same liquid would also bounce, and (2) D_c would increase notably with T_p because more vapor would be generated in the $L1$ and $L2$ zones [and this is not the case as it was shown in Fig. 4(e)].

A quantitative attempt to estimate the vapor produced in each zone and the coalescence size can be found in the Supplemental Material [36]. Here, we provide direct evidence of the existence of the $L3$ vapor layer. To produce visible amounts of vapor during the collision time, we used liquids with the largest ΔT_B and a Drop 2 of the most volatile liquid (lowest latent heat). Based on Table I [36], we choose ethylene glycol ($T_{B1} = 190\,^{\circ}\mathrm{C}$) and chloroform ($T_{B2} = 54\,^{\circ}\mathrm{C}$, $L = 247$ kJ/kg). Figure 5(b) shows snapshots of the collision (see also Supplemental Material movie [36]). Clearly, a vapor layer is produced between the drops at the moment of collision, which prevents coalescence. The same mechanism is probably behind the frustrated coalescence for other pairs of liquids, but the vapor produced is scarce and cannot be easily visualized. When the smaller droplet decreases in size after several bounces and becomes spherical (i.e., $D_2 \sim \lambda_c$), the vapor layer can be evacuated during the collision time and the drops finally coalesce. When this happens, different situations occur: for ethylene glycol and chloroform, ΔT_B is so large that chloroform explodes violently [Fig. 5(c)]. For immiscible liquids, for instance water and toluene, the drops merge in a single Leidenfrost drop, but they remain unmixed with toluene covering the water drop [Fig. 5(d)]. Methylene blue in water allows us to confirm that there is no mass transfer between the droplets. This contrasts with miscible drops [Fig. 1(d)], where the transparent droplet becomes bluish only milliseconds after coalescence.

In summary, this is the first study focused on the collision outcome of Leidenfrost drops of distinct miscible and immiscible liquids. The results are remarkably different from those observed with drops at room temperature. The

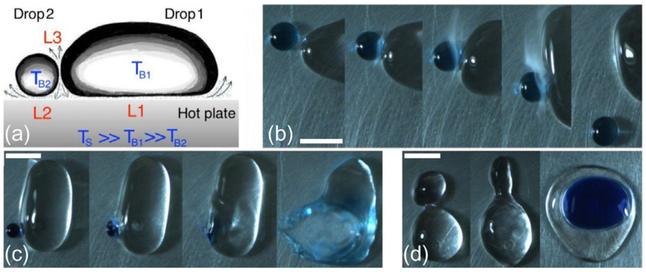

FIG. 5. (a) Sketch of the triple Leidenfrost effect (see text). (b) Snapshots taken at 500 fps showing the vapor layer generated when droplets of ethylene glycol (transparent) and chloroform (blue) collide ($T_p = 350\,^{\circ}\mathrm{C}$). (c) Explosive coalescence of chloroform (blue) with ethylene glycol. (d) Together but not scrambled: water (blue) and toluene join but remain unmixed because these liquids are immiscible (scale bars = 5 mm).

underlying mechanism could be applied for selective coalescence (see Supplemental Material movie [36]), for drops manipulation in millimetric fluidic systems [26], and to understand fuel drops interaction in overheated engines [20–22].

Research supported by Conacyt Mexico through Frontier Science Project 140604, FORDECYT-PRONACES, and Cátedra Marcos Moshinsky 2020. We thank J. Pierron and L. Vallet for initial tests.

---

[*]Corresponding author.
fpacheco@ifuap.buap.mx
[†]Corresponding author.
rledesmaalonso@gmail.com

[1] J. G. Leidenfrost, *De Aquae Communis Nonnullis Qualitatibus Tractatus* (Duisburg, 1756).
[2] A.-L. Biance, C. Clanet, and D. Quéré, Phys. Fluids **15**, 1632 (2003).
[3] N. Nagai and S. Nishio, Exp. Therm. Fluid. Sci. **12**, 373 (1996).
[4] H. Kim, B. Truong, J. Buongiorno, and L.-W. Hu, Appl. Phys. Lett. **98**, 083121 (2011).
[5] I. U. Vakarelski, N. A. Patankar, J. O. Marston, D. Y. C. Chan, and S. T. Thoroddsen, Nature (London) **489**, 274 (2012).
[6] J. D. Bernardin and I. Mudawar, J. Heat Transfer **124**, 864 (2002).
[7] S. Hidalgo-Caballero, Y. Escobar-Ortega, and F. Pacheco-Vázquez, Phys. Rev. Fluids **1**, 051902(R) (2016).
[8] L. Maquet, B. Sobac, B. Darbois-Texier, A. Duchesne, M. Brandenbourger, A. Rednikov, P. Colinet, and S. Dorbolo, Phys. Rev. Fluids **1**, 053902 (2016).
[9] G. Lagubeau, M. Le Merrer, C. Clanet, and D. Quéré, Nat. Phys. **7**, 395 (2011).
[10] S. R. Waitukaitis, A. Zuiderwijk, A. Souslov, C. Coulais, and M. Van Hecke, Nat. Phys. **13**, 1095 (2017).
[11] C. Liu, K. Sun, C. Lu, J. Su, L. Han, Z. Wang, and Y. Liu, J. Colloid Interface Sci. **569**, 229 (2020).
[12] G. Graeber, K. Regulagadda, P. Hodel, C. Kuttel, D. Landolf, T. M. Schutzius, and D. Poulikakos, Nat. Commun. **12**, 1727 (2021).
[13] P. Agrawal, G. G. Wells, R. Ledesma-Aguilar, G. McHale, A. Buchoux, A. Stokes, and K. Sefiane, Appl. Energy **240**, 399 (2019).
[14] A. Bouillant, T. Mouterde, P. Bourrianne, A. Lagarde, C. Clanet, and D. Quéré, Nat. Phys. **14**, 1188 (2018).
[15] X. Ma, J.-J. Lietor-Santos, and J. C. Burton, Phys. Fluids **27**, 091109 (2015).
[16] P. Yi, P. Thurgood, N. Nguyen, H. Abdelwahab, P. Petersen, C. Gilliam, K. Ghorbani, E. Pirogova, S.-Y. Tang, and K. Khoshmanesh, Soft Matter **16**, 8854 (2020).
[17] J. O. Marston, I. U. Vakarelski, and S. T. Thoroddsen, J. Fluid Mech. **699**, 465 (2012).
[18] F. Moreau, P. Colinet, and S. Dorbolo, Phys. Rev. Fluids **4**, 013602 (2019).
[19] Although droplets of distinct liquids interact on overheated surfaces in several processes (e.g., fuel-oxidizer spray systems and composite fuels combustion [20–22]), the collision outcome for two Leidenfrost droplets of unlike liquids remained so far unexplored.
[20] S. Sen, V. Vaikuntanathan, and D. Sivakumar, Int. J. Thermal Sci. **121**, 99 (2017).
[21] C. Cen, H. Wu, C. Lee, L. Fan, and F. Liu, Intl. J. Heat Mass Transfer **132**, 130 (2019).
[22] A. E. Ashikhmin, N. A. Khomutov, M. V. Piskunov, and V. A. Yanovsky, Appl. Sci. **10**, 685 (2020).
[23] J. Qian and C. K. Law, J. Fluid Mech. **331**, 59 (1997).
[24] C. Tang, P. Zhang, and C. K. Law, Phys. Fluids **24**, 022101 (2012).
[25] K. G. Krishnan and E. Loth, Int. J. Multiphase Flow **77**, 171 (2015).
[26] J. Jin, C. Ooi, D. Dao, and N.-T. Nguyen, Micromachines **8**, 336 (2017).
[27] K. H. Al-Dirawi and A. E. Bayly, Exp. Fluids **61**, 50 (2020).
[28] J.-T. Zhang, H.-R. Liu, and H. Ding, Phys. Fluids **32**, 082106 (2020);
[29] T.-C. Gao, R.-H. Chen, J.-Y. Pu, and T.-H. Lin, Exp. Fluids **38**, 731 (2005).
[30] R.-H. Chen and C.-T. Chen, Exp. Fluids **41**, 453 (2006).
[31] J. B. Boreyko and C.-H. Chen, Phys. Fluids **22**, 091110 (2010).
[32] O. Ramírez-Soto, V. Sanjay, D. Lohse, J. T. Pham, and D. Vollmer, Sci. Adv. **6**, eaba4330 (2020).
[33] N. Yi, B. Huang, L. Dong, X. Quan, F. Hong, P. Tao, C. Song, W. Shang, and T. Deng, Sci. Rep. **4**, 4303 (2014).
[34] F. Liu, G. Ghigliotti, J. J. Feng, and C.-H. Chen, J. Fluid Mech. **752**, 22 (2014).
[35] N. E. Shlegel, P. P. Tkachenko, and P. A. Strizhak, Powder Technol. **367**, 820 (2020).
[36] See Supplemental Material at http://link.aps.org/supplemental/10.1103/PhysRevLett.127.204501 for more information about the liquids properties, and the analysis of the evaporation rate for single and colliding droplets, which includes Refs. [2,8,37–42]. See also movie of two Leidenfrost drops collisions for different liquids combinations.
[37] Merck KGaA. Merck solvent miscibility chart (2020) https://www.sigmaaldrich.com/chemistry/solvents/solvent-miscibility-table.html, last accessed 01 December 2020.
[38] G. Vázquez, E. Alvarez, and J. M. Navaza, J. Chem. Eng. Data **40**, 611 (1995).
[39] C. L. Yaws, *Chemical Properties Handbook* (McGraw-Hill Education, New York, 1999).
[40] Engineering ToolBox (2001), https://www.engineeringtoolbox.com.
[41] B. Sobac, A. Rednikov, S. Dorbolo, and P. Colinet, *Droplet Wetting and Evaporation* (Academic Press, New York, 2015), pp. 85–99.
[42] T. R. Cousins, R. E. Goldstein, J. W. Jaworski, and A. I. Pesci, J. Fluid Mech. **696**, 215 (2012).
[43] M.-A. J. van Limbeek, O. Ramírez-Soto, A. Prosperetti, and D. Lohse, Soft Matter **17**, 3207 (2021).
[44] Results obtained with drops of diameter $D > \lambda_c$.
[45] At this temperature, all the liquids listed in Table I exhibit Leidenfrost state on the aluminum plate.
[46] For dimethylformamide(DMF)-water ($\Delta T_B \sim -53\,^{\circ}\mathrm{C}$), it is the water drop the one that could reach the Leidenfrost state interacting with DMF, but the latent heat of water is so high that the vapor produced during the collision time is probably not enough to prevent coalescence.